

RESEARCH

Open Access



Stratification of human gut microbiomes by succinotype is associated with inflammatory bowel disease status

Laura Anthamatten^{1,2}, Philipp Rogalla von Bieberstein¹ , Carmen Menzi¹ , Janina N. Zünd² , Christophe Lacroix² , Tomas de Wouters^{1*} and Gabriel E. Leventhal^{1*}

Abstract

Background The human gut microbiome produces and consumes a variety of compounds that interact with the host and impact health. Succinate is of particular interest as it intersects with both host and microbiome metabolism. However, which gut bacteria are most responsible for the consumption of intestinal succinate is poorly understood.

Results We build upon an enrichment-based whole fecal sample culturing approach and identify two main bacterial taxa that are responsible for succinate consumption in the human intestinal microbiome, *Phascolarctobacterium* and *Dialister*. These two taxa have the hallmark of a functional guild and are strongly mutual exclusive across 21,459 fecal samples in 94 cohorts and can thus be used to assign a robust “succinotype” to an individual. We show that they differ with respect to their rate of succinate consumption in vitro and that this is associated with higher concentrations of fecal succinate. Finally, individuals suffering from inflammatory bowel disease (IBD) are more likely to have the *Dialister* succinotype compared to healthy subjects.

Conclusions We identified that only two bacterial genera are the key succinate consumers in human gut microbiome, despite the fact that many more intestinal bacteria encode for the succinate pathway. This highlights the importance of phenotypic assays in functionally profiling intestinal microbiota. A stratification based on “succinotype” is to our knowledge the first function-based classification of human intestinal microbiota. The association of succinotype with IBD thus builds a bridge between microbiome function and IBD pathophysiology related to succinate homeostasis.

Introduction

The intestinal microbiome interacts with its host through the production and consumption of physiologically relevant metabolites [1]. This overall microbiome metabolic activity emerges from the individual activity of the member microbes, and thus the overall metabolic output can vary depending on the specific microbiome composition [2]. Screening for and controlling the specific microbes that are the drivers of these activities is a promising diagnostic and intervention target. However, which

*Correspondence:

Tomas de Wouters
t.dewouters@pharmabiome.com
Gabriel E. Leventhal
g.leventhal@pharmabiome.com

¹ PharmaBiome AG, Schlieren, Switzerland

² Laboratory of Food Biotechnology, Institute of Food, Nutrition and Health, ETH Zurich, Zurich, Switzerland



© The Author(s) 2024. **Open Access** This article is licensed under a Creative Commons Attribution-NonCommercial-NoDerivatives 4.0 International License, which permits any non-commercial use, sharing, distribution and reproduction in any medium or format, as long as you give appropriate credit to the original author(s) and the source, provide a link to the Creative Commons licence, and indicate if you modified the licensed material. You do not have permission under this licence to share adapted material derived from this article or parts of it. The images or other third party material in this article are included in the article's Creative Commons licence, unless indicated otherwise in a credit line to the material. If material is not included in the article's Creative Commons licence and your intended use is not permitted by statutory regulation or exceeds the permitted use, you will need to obtain permission directly from the copyright holder. To view a copy of this licence, visit <http://creativecommons.org/licenses/by-nc-nd/4.0/>.

specific microbe in a microbiome is the key responsible for a specific function remains largely unknown.

Some metabolites—like succinate—are produced and consumed by both the microbiome and the host. On the host side, succinate is a key intermediate of the tricarboxylic acid cycle and thus intricately related to host metabolic homeostasis. On the microbiome side, succinate is an intermediate product of anaerobic carbohydrate fermentation and thus related to microbial energy production [3]. This intersection of host and microbiome metabolism poses a challenge for host regulation: while the host might attempt to regulate how succinate is produced and used, its regulatory control does not expand to the microbiome. As a result, disruptions in how succinate is produced and consumed by the microbiome can have a multifaceted impact on the host. In a healthy gut, succinate is rapidly converted into propionate [4–6], which in turn is readily absorbed by the host epithelium [7]. However, elevated concentrations of succinate measured in human feces have been associated with intestinal inflammation [8–11], suggesting a pro-inflammatory effect of excess circulating succinate. Consequently, microbes that metabolize succinate have been suggested to alleviate this inflammatory effect [12, 13].

Only few bacteria are known to anaerobically consume succinate. Various intestinal bacteria—including for example many *Bacteroidaceae*—produce propionate from sugars via the succinate pathway [14, 15] and in some cases export the intermediate succinate due to the low energetic yield of converting succinate to propionate [16]. But these succinate producers have generally not been observed to take up and convert succinate when supplied extracellularly. Succinate can also be otherwise utilized by select bacteria. For example, *Veillonella parvula* can decarboxylate succinate during lactate consumption to produce propionate and increase growth yield [17], and *Clostridioides difficile* can convert succinate to butyrate to rebalance NADH. However, a substantial consumption of extracellular succinate has only been demonstrated for isolates of the *Negativicutes*, including *Phascolarctobacterium* spp. [4, 18] and *Dialister* spp. [19–21]. Overall, the degree to which these different taxa and pathways are active in the human intestine remains poorly understood.

Here, we aimed to identify and characterize the key bacteria involved in human intestinal succinate consumption. In previous work, we showed that some human fecal microbiomes were able to consume succinate within 48 h of in vitro cultivation and that this mapped to the presence or absence of certain *Negativicutes* bacteria [22]. We first expanded upon this approach to differentiate between succinate consumption that takes more than 48 h and an overall absence of the function. We observed that all fecal microbiomes had the capacity to consume succinate but did differ in the rate at which they did so.

We then verified that the succinate consumption rate in pure culture mapped to the consumption rate of the whole fecal sample. Our data suggest that bacteria from the genera *Phascolarctobacterium* and *Dialister* are the dominant succinate consumers in the human GI tract but that *Phascolarctobacterium* converts succinate to propionate significantly more rapidly than *Dialister*. We then analyzed publicly available cohorts of human fecal microbiota to show that *Phascolarctobacterium* and *Dialister* are typically mutually exclusive in human microbiomes and that IBD patients significantly more likely to have *Dialister* as their dominant succinate consumer compared to healthy individuals. We thus propose that the slower rate of succinate consumption by *Dialister* in the human intestine could be an important contributor to the pathogenesis of intestinal inflammation.

Results

Human gut microbiota differ in their ability and rate to metabolize succinate in vitro

To understand succinate consumption in complex intestinal microbiota, we performed in vitro enrichments of feces from 13 different human donors akin to what is described in Anthamatten et al. [22]. Briefly, we inoculated diluted fecal samples in triplicate into a defined base medium either supplemented with 30 mM of succinate as main carbon source or a non-supplemented control and measured (i) how much of succinate was consumed after 2 and 7 days of strict anaerobic cultivation and (ii) what metabolites were produced in return (Fig. 1a). Because of the stochasticity with respect to diluted inoculum composition, we analyzed each replicate independently.

The time required to consume the supplied succinate differed between enrichment cultures (Fig. 1b), with all of the supplied succinate consumed within 48 h in some enrichments and no succinate consumed in others after 7 days. We thus classified the enrichments into four categories as a function of their succinate consumption: “fast,” “intermediate,” “slow,” and “non-consumers.” Fast enrichments consumed > 90% of the supplied succinate within the first 48 h of cultivation ($n = 11/39$), intermediate enrichments consumed > 90% within 7 days (10/39), slow enrichments consumed between 20 and 90% within 7 days (6/39), and non-consuming enrichments consumed < 20% within 7 days (12/39). Enrichments inoculated with the same fecal sample were generally consistent in terms of category, with M1 to M4 fast, M5 intermediate, M6 and M7 slow, and M8 to M13 non-consumers, although we did observe differences in the categories between replicates. This suggests that specific properties of the fecal sample contribute—at least in part—to the category of succinate consumption, for example specific taxa or different metabolic pathways. The optical density at 48 h was

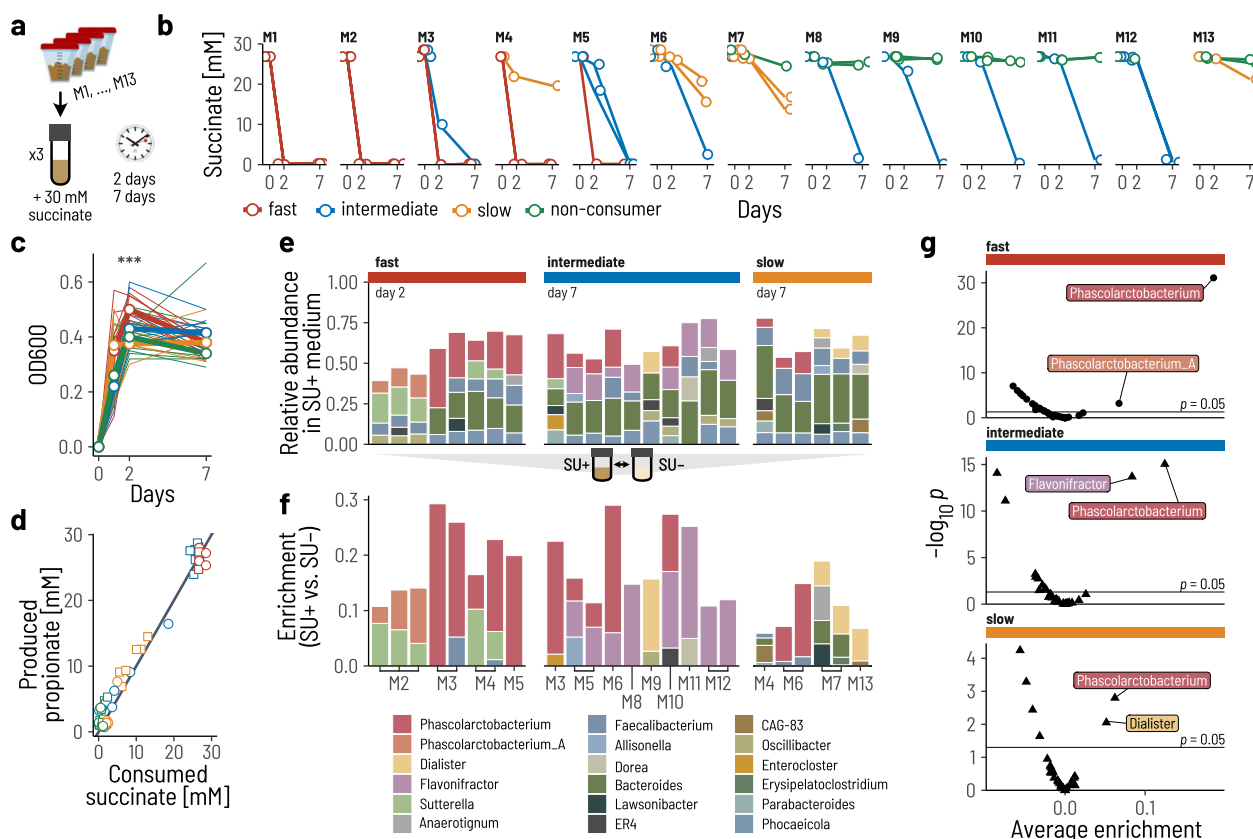


Fig. 1 Fecal microbiomes consume succinate at different rates. **a** We performed enrichment cultures of whole fecal microbiota from 13 different donors in a basal medium supplemented with 30 mM succinate as the primary carbon source. The triplicate cultures were sampled after 2 and 7 days, respectively. **b** The supplied succinate is consumed differently across fecal microbiota and replicates. We classify a culture as fast (red), intermediate (blue), or slow (orange) consumer, or non-consumer (green) of succinate. Each circle is a measurement of the succinate concentration in a replicate enrichment. The lines connect multiple time points from the same replicate. **c** The increase in optical density (OD) at day 2 was highest for the fast consuming cultures. Each thin line is a replicate enrichment from **(b)** and the thick lines are the average in each class. **d** The consumed succinate was converted to propionate at a molar ratio of 1:1. Each point corresponds to a point in **(b)**. **e** Genus-level composition of the enrichment cultures after either 2 or 7 days. Only genera with at least 5% relative abundance are shown. **f** The “enrichment” is the difference in relative abundance between enrichments with supplemented succinate (SU+) and the corresponding enrichment without supplemented succinate (SU-) of the same donor. Only genera with positive enrichment values are shown. **g** Coefficients from a linear regression of the enrichment value on the rate category for each genus. Only genera with positive estimates are shown. Filled boxes are estimates with $p < 0.05$

higher in the fast enrichments compared to the other categories (Fig. 1c; Kruskal-Wallis test, $p = 0.0004$), further indicating that different bacteria or even pathways might be associated with the category of succinate consumption. However, succinate was converted to propionate at a molar ratio of 1:1 across all enrichments (Fig. 1d) as expected from the succinate pathway [14], suggesting that this same pathway was “in use” across fecal microbiomes.

We thus next set out to determine which bacterial taxa were performing the conversion of succinate to propionate across enrichments. To this end, we performed 16S amplicon sequencing of the succinate enrichment cultures (SU+) and the control cultures (SU-) on days 2 and 7 and computed the differential increase of each genus in

SU+ compared to the SU- (see the “Methods” section). Some typically abundant genera dominated the enrichment cultures irrespective of the consumption category, including for example *Bacteroides*, *Phocaeicola*, or *Faecalibacterium* (Fig. 1e). To pinpoint those taxa that were specifically associated with succinate consumption across the three categories, we focused on those genera that had an increase in relative abundance in the SU+ compared to the SU- cultures (Fig. 1f).

Four bacterial genera were significantly associated with the different consumption categories. We performed a linear regression of enrichment in SU+ versus SU- and identified those genera that were significantly associated with at least one of the categories (Fig. 1g). *Phascolarctobacterium*

and *Phascolarctobacterium_A* were most strongly associated with the fast category, *Phascolarctobacterium* and *Flavonifractor* with the intermediate category, and *Phascolarctobacterium* and *Dialister* with the slow category. Of the four identified putative succinate consuming taxa, only one was typically dominant in any one specific enrichment. These data imply that these four genera are most likely those that are responsible for succinate consumption in the enrichments.

Representative genomes of each of these four genera all contained the gene cluster for succinate to propionate conversion first described in *Veillonella parvula*, starting from the succinate-CoA transferase to the methylmalonyl-CoA decarboxylase (Supplementary Figure S1a). The methylmalonyl-CoA decarboxylase subunit alpha (*mmdA*) has previously been used as a marker gene for the succinate pathway [14]. We wanted to know whether *mmdA* gene similarity was a good predictor for succinate consumption. To answer this, we reconstructed the phylogenetic tree of *mmdA* sequences from GTDB and tested a selection of isolates from along the tree for their ability to consume succinate (Supplementary Figure S1b). All the four genera identified in the enrichments could consume succinate in monoculture in the same in vitro conditions (Supplementary Figure S1c). However, the majority of the other tested isolates did not consume meaningful amounts of succinate, despite closely related *mmdA* genes (Supplementary Figure S1c). This suggests that the presence of a homologous *mmdA* gene—or even the complete succinate pathway as in many *Bacteroidetes*—is not sufficient to confer the ability to consume extracellular succinate in the tested conditions. Together with the fecal enrichments, these results suggest that extracellular succinate consumption in human fecal samples is constrained to very few taxa that include the four genera identified here.

Intestinal succinate-consuming bacteria differ in their succinate conversion rate

The in vitro enrichments essentially test for the competitive ability of the bacteria that comprise the fecal microbiota for succinate. The outcome of such a competition is influenced by two key factors: (i) the per capita rate at which the taxa consume succinate and (ii) the population size of each taxon in the inoculum.

To test whether the identified taxa differ in their per capita succinate consumption rate, we performed in vitro cultures of eleven representative isolates in a growth medium supplemented with 80 mM succinate and measured the decrease in succinate concentration and the resulting bacterial growth over time (Fig. 2a). The representative isolates included two from the genus *Dialister* (*D. hominis* and *D. invisus*), four from *Phascolarctobacterium* (4x *P. faecium*), one from *Phascolarctobacterium_A* (*P. succinatutens*), and

three from the genus *Flavonifractor* (3x *F. plautii*). We then estimated the succinate consumption rates of each isolate by deriving a substrate consumption and growth model and subsequently fitting it to the succinate concentration and optical density data in a Bayesian framework (Fig. 2a and the “Methods” section).

The mathematical model provided a good fit to the experimental data for the *Dialister*, *Phascolarctobacterium*, and *Phascolarctobacterium_A* isolates (Fig. 2b and Supplementary Figure S2). This confirms that these bacteria directly use the energy from converting succinate to propionate for growth. In contrast, the model was not a good fit to the data for *Flavonifractor* for which we observed diauxic growth with a first phase without appreciable succinate consumption (Supplementary Figure S3). To account for this diauxie, we expanded the model to include a second preferred but unobserved growth substrate (Fig. 2a). Only once this substrate was depleted does succinate consumption start. This updated model proved a much better fit to the data (Fig. 2b and Supplementary Figure S3). With the estimated model parameters at hand, we then compared the strains based on their *per capita* succinate consumption rate.

The estimated succinate uptake rates were consistent within genera but differed strongly between genera (Fig. 2c). *Phascolarctobacterium* strains consumed succinate at twice the rate compared to *Dialister* strains, with 63.7 mM/h/OD on average and 30.7 mM/h/OD on average, respectively. This translates to longer times required to consume all of the supplemented succinate for the *Dialister* cultures compared to the *Phascolarctobacterium* cultures given equal inoculum densities. *Flavonifractor* strains had an even lower uptake rate, with 11.5 mM/h/OD on average. However, this did not translate to substantially longer times required to consume the supplied succinate because the *Flavonifractor* cultures first grew on an alternative preferred resource and thus initiate succinate consumption at substantially larger cell densities. This can explain why *Flavonifractor* is more strongly enriched in the fecal microbiomes M8-M12 compared to *Dialister* despite slower *per capita* uptake rate. Overall, these results confirm that the observed differences in the rate of succinate consumption between the whole fecal microbiomes can be mapped to differences in uptake rates of the succinate consuming bacteria.

Having demonstrated that the succinate consumption rate differs between taxa, we next asked to what degree the starting abundances of the succinate consumers might have impacted the overall consumption rate. We thus quantified the relative abundance of the four genera in the thirteen fecal microbiota.

The three genera *Phascolarctobacterium*, *Phascolarctobacterium_A*, and *Dialister* followed a

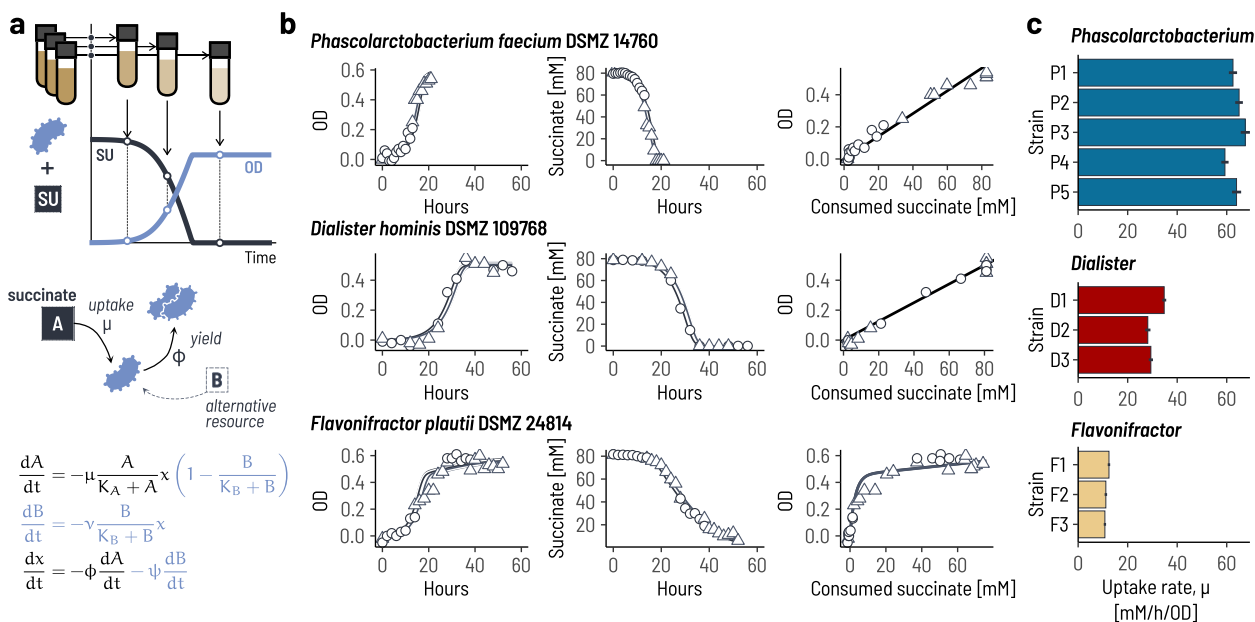


Fig. 2 Succinate-consuming gut bacteria differ in their succinate uptake rate. **a** To estimate the rate at which different representative isolates consume succinate, we performed replicate cultures of a panel of eleven isolates in media supplemented with 80 mM of succinate as the primary carbon source. Each replicate culture was destructively sampled at a different time point between 0 and 60 h. We then estimated the succinate uptake rate by fitting a mathematical model of succinate uptake and growth to the data. We accounted for the observed diauxic growth of *Flavonifractor* sp. by adding a second (unobserved) resource to the model (blue terms). **b** Experimental data and model fits for one representative isolate of each genus. For each isolate, two biological replicate “sets” were inoculated (circles and triangles). Initial bacterial concentrations, x_0 , and succinate concentrations, A_0 , were estimated separately for each replicate set and are shown as separate lines. Data for *Flavonifractor* isolates used the diauxic model. **c** Posterior mean estimates (bars) and 90% highest-probability density intervals (black lines) for the eleven strains. P1: *P. faecium* DSMZ 14760; P2: *P. faecium* PB-SDVAP; P3: *P. faecium* PB-SJWFW; P4: *P. faecium* PB-SPUPY; P5: *P. succinatutens* DSMZ 22533; D1: *D. hominis* DSMZ 109768; D2: *D. invisus* PB-SARUR; D3: *D. succinatiphilus* DSMZ 21274; F1: *F. plautii* DSMZ 24814; F2: *F. plautii* PB-SCBYV; F3: *F. plautii* PB-SSJQB

different compositional pattern than *Flavonifractor* (Fig. 3a). The former three all had a bimodal abundance distribution in the fecal samples and were either present at 1–7% or otherwise undetectable. In contrast, *Flavonifractor* was detected in all thirteen fecal microbiota at a consistent abundance of 0.01–0.4%. Because *Flavonifractor* only consumes succinate as a secondary preference, we hypothesized that the bimodal prevalence of the three “primary” consuming genera was the result of mutual exclusion from strong substrate competition. If this was the case, then each fecal sample should only harbor one of the three consumers. Indeed, each of the thirteen fecal microbiota only had one dominant primary succinate consumer (Fig. 3b), in most cases with full mutual exclusion (at the sensitivity of sequencing), and this pattern of mutual exclusion also occurred at the species (Fig. 3c) and ASV level (Supplementary Figure S4).

The clear association between the dominant primary succinate consumer and inoculum microbiota indicates that different human intestinal microbiota might be well-classified by the identity of their primary succinate degrader: their “succinotype.” Based on the patterns

observed here, we introduce the “P” and “D” succinotypes for fecal microbiota that have either *Phascolarctobacterium*/*Phascolarctobacterium_A* or *Dialister*, respectively (Fig. 3c). For the P succinotype, we grouped the two genera together because of both their phylogenetic proximity and similarity in per capita uptake rate. We next asked whether such a classification of human microbiomes into succinotypes was robust beyond the 13 tested fecal microbiota.

Succinotypes appear broadly across human cohorts and are associated with disease

To test whether our classification of succinotypes was generalizable to fecal human microbiota more broadly, we analyzed nine publicly available cohorts of 16S amplicon human fecal microbiome data comprising a total of 11,885 samples [23–27]. Furthermore, we also analyzed 85 cohorts with shotgun metagenomic data from the curatedMetagenomicData collection [28]. We used a consistent taxonomic classification based on the Genome Taxonomy Database (GTDB r95) [29].

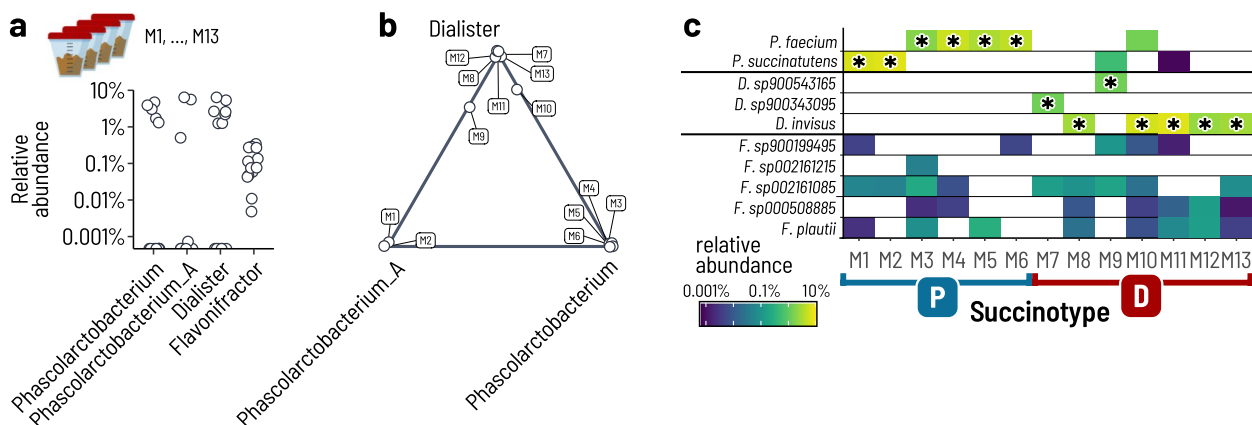


Fig. 3 Human fecal microbiota can be classified into “succinotypes” based on their dominant succinate consuming bacterium. **a** Relative abundances of the four identified succinate consuming genera in the fecal microbiota. **b** The three genera *Phascolarctobacterium*, *Phascolarctobacterium_A*, and *Dialister* are strongly mutually exclusive. The position in the ternary diagram shows the relative abundance of the three genera in each of the fecal microbiota. Points in the corners indicate full mutual exclusivity. **c** Relative abundances of the succinate consuming taxa in the fecal microbiota resolved at the species level. The asterisk indicates the dominant species in a fecal microbiota. We assign fecal microbiota with a dominant *Phascolarctobacterium*, *Phascolarctobacterium_A* to a succinotype “P” and those with a dominant *Dialister* to a succinotype “D”

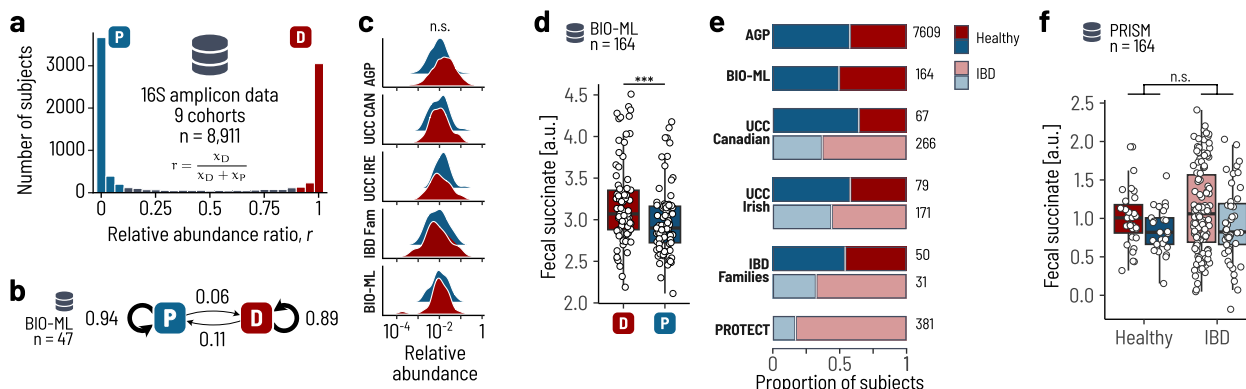


Fig. 4 Clear succinotypes are found broadly and are associated with disease. **a** The distribution of the relative abundance ratio of *Dialister* (D) compared to *Phascolarctobacterium*/*Phascolarctobacterium_A* (P) in fecal samples is strongly bimodal. The histogram encompasses 9 pooled cohorts of 16S amplicon data with a total of 8911 individuals. **b** Transition probabilities between succinotypes over time estimated individuals with repeat samples in the BIO-ML cohort. **c** Distribution of relative abundances of D (red) and P (blue) in the fecal samples of healthy individuals. There is no significant difference between D and P across cohorts. **d** Succinate concentrations in fecal samples from the BIO-ML cohort (Mann-Whitney *U* test, $p = 0.001619$). **e** Fraction of subjects assigned the D and P succinotype across cohorts and disease status. Dark colors are healthy subjects and light colors are IBD patients. **f** Succinate concentrations in fecal samples from the PRISM cohort. There are no significant differences in fecal succinate between healthy subjects and IBD patients. AGP: American Gut Project; UCC CAN: UCC Canadian Cohort; UCC IRE: UCC Irish Cohort; IBD Fam: IBD Families Cohort; BIO-ML: Broad Institute-OpenBiome Microbiome Library

The majority of individuals across all cohorts had a well-defined succinotype. Most samples in the amplicon data (91.3%) had detectable abundances of either *Dialister* or *Phascolarctobacterium*, with slightly lower proportions in the shotgun data (76.9%). In order to robustly assign a succinotype, we set either a threshold of at least 10 reads assigned to either D or P (when counts were available) or otherwise a combined relative abundance of at least 0.01%. We retained 8911 samples after pruning multiple samples from the same subject. We then computed

the abundance fraction, $r = x_D / (x_D + x_P)$, where the x are the abundances of D and P, respectively. The vast majority of samples had r values that were close to 0 or 1, respectively (Fig. 4a, Supplementary Figure S6). We thus assigned a succinotype when the abundance of D was at least ten times higher than P, and *vice versa*, that is $r < 0.1$ or $r > 0.9$. Doing so, we were able to assign clear succinotypes to 7,653 (85.6%) of the retained amplicon samples and 11,442 (91.2%) of the retained shotgun samples.

We next asked whether the assignment of succinotypes to individuals remained stable over time using two of the cohorts. The Broad Institute-OpenBiome Microbiome Library (BIO-ML) and the Health Practitioners Follow-up Study (HPFS) comprise individuals that were sampled more than once. From these data, we computed the transition probabilities between succinotypes, that is, the fraction of times an individual changed its succinotypes from D to P or vice versa. In BIO-ML, individuals retained the same succinotype in the subsequent fecal sample 88.9% and 94.4% of the time for D and P, respectively (Fig. 4b), and the same was confirmed in the HPFS study (92% and 94%, Supplementary Figure S6). This demonstrates that individuals can be robustly classified into either a “D” or “P” succinotype based on their cross-sectional microbiome composition.

The relative abundance of the succinate utilizers did not differ between healthy individuals with different succinotypes. For each healthy subject, we computed the total relative abundance of succinate utilizers as the sum of relative abundances of D and P. The succinate utilizers had a mean relative abundance of 1.14%, with a 95% of the samples between 0.11 and 12.0% (Fig. 4c). We tested for a difference in relative abundance of the succinate utilizers between individuals that were assigned to either succinotype. To account for potential variability between datasets, we used a mixed-effects model with random slopes and intercepts for the succinotype across cohorts. There was no consistent significant effect of succinotype on the log relative abundance ($p = 0.503$). This implies that the size of the “succinate utilization niche” is conserved and hence does not depend on the identity of the taxon that occupies the niche.

We hypothesized that the lower rate of succinate consumption by *Dialister* as compared to *Phascolarctobacterium* would imply that the net concentration of succinate is higher in D-type as compared to P-type individuals. To test this, we used the metabolomic data from the BIO-ML cohort. Fecal succinate concentrations were significantly higher in D-types compared to P-types (Mann-Whitney U test, $p = 0.001619$; Fig. 4d), and there was no significant effect of the relative abundance of succinate utilizers in a linear model including both succinotype and relative abundance ($p = 0.559$, Supplementary Figure S7). These results support the notion that the niche size of succinate consumption does not differ between succinotypes, but that the slower removal of succinate by *Dialister* manifests as a higher net succinate concentration.

Given these increased levels of intestinal succinate and the reported role of succinate in inflammation [3], we hypothesized that a *Dialister* succinotype would be more prone to intestinal inflammation—and possibly at higher risk of inflammatory bowel disease (IBD). We tested for

an effect of succinotype on IBD status using all cohorts in a logistic regression on succinotype with cohort as a random effect.

IBD patients were consistently more likely to be D-types than P-types (Fig. 4e). The odds ratio of IBD versus healthy was 2.2 times lower for P-types compared to D-types (logit regression, $\beta = -0.805$, CI = $[-1.16, -0.449]$, $p = 9.27 \cdot 10^{-6}$). We thus asked whether succinate concentrations are disproportionately higher in D-type IBD patients than P-types using the metabolomic data from the PRISM cohort [30], for which taxonomic composition based on shotgun metagenomic data paired with metabolomic data were available [31]. Consistent with the data from BIO-ML, fecal succinate concentrations were higher in D-types than in P-types, but the difference was not significantly different from that in healthy individuals (Fig. 4f; two-way ANOVA, $F_{IBD}(1, 217) = 2.32$, $p_{IBD} = 0.12$, $F_{Stype}(1, 217) = 6.29$, $p_{Stype} = 0.013$). Overall, this suggests that the *Dialister* succinotype contributes in some manner to IBD pathogenesis, likely as the result of its slower consumption of succinate.

Finally, to check to which extent the association of succinotypes with disease was specific to IBD, we looked at the succinotype distributions in a set of other diseases that were part of the curatedMetagenomicDatasets package. Two diseases, colorectal cancer (CRC) and atherosclerotic cardiovascular disease (ACVD), were associated with the P succinotype (Supplementary Figure S8). However, none of the other tested diseases were significantly associated with the D succinotype, indeed suggesting a specific role of high *Dialister* or low *Phascolarctobacterium* in IBD.

Discussion

The goal of this study was to map out which human intestinal bacteria are the main consumers of succinate—a metabolite that is at a key crossroad of human and microbiome metabolism. Our multi-faceted analysis of fecal microbiota and bacterial isolates identified two bacterial taxonomic groups as key succinate consumers in human intestinal microbiomes, *Phascolarctobacterium* and *Dialister*. These two taxa are highly mutually exclusive in fecal microbiomes of western populations, allowing for the clear classification of individuals into P and D “succinotypes.” These succinotypes differ with respect to their succinate consumption rate, with the D types consuming succinate more slowly than the P-succinotypes, and this translates to higher fecal concentrations of succinate. Finally, while the prevalence of succinotypes in healthy populations is rather balanced, IBD patients are significantly more likely to have a D-succinotype than a P-succinotype. This provides evidence for an imbalance

between host and microbiota succinate metabolism in intestinal inflammatory diseases like IBD.

The discovery that only two taxonomic groups occupy the succinate niche in human intestinal microbiota is strikingly simple and somewhat unexpected given the wider diversity of intestinal bacteria that have been reported to consume succinate. These include, for example, *Clostridioides difficile* and *Clostridium kluyveri* that convert succinate to butyrate [32, 33] or *Veillonella parvula* that decarboxylates succinate during lactate consumption [17]. However, these bacteria do not *per se* use succinate as a growth substrate, with the former two regenerating NAD⁺ and the latter increasing growth yield from lactate but not able to grow on succinate alone. This might be similar to how *Flavonifractor plautii* uses succinate in our data, with a comparatively low per capita consumption rate. In contrast, *Phascolarctobacterium* and *Dialister* generate energy for growth from the decarboxylation of succinate. Yet, because the energetic yield of converting succinate to propionate is low [34], there is limited selection pressure for bacteria to specialize on succinate consumption. This is further illustrated by those bacteria that encode the full succinate pathway, like *Bacteroides* sp., but mostly favor cutting short and excreting succinate instead of fully running the pathway to produce propionate [35]. Using succinate as a growth substrate has been observed for other taxa, including *Propionigenium modestum* [36] and *Peptostreptococcus* sp. [34], but given that (a) *Phascolarctobacterium* and *Dialister* are de facto fully mutually exclusive and (b) the prevalence of either is close to 100% in humans, we posit that these two taxonomic groups have specialized specifically on succinate consumption in the human intestine. What the evolutionary process was that resulted in this arrangement, and whether there is more fine-scale strain-level diversity also within the two genera remains to be investigated.

It is also surprising, based on our results, that D-succinotypes are stable and are not invaded by *Phascolarctobacterium*, given that its higher per capita succinate consumption rate should impart a fitness advantage over *Dialister*. We do note that a small minority of subjects in our fecal enrichments and also the public data have mixed succinotypes with comparable abundances of *Dialister* and *Phascolarctobacterium*. Whether these are snapshots of a transient shift from one succinotype to the other and more generally what the ecological forces are that stably maintain a succinotype in an individual over time is yet to be uncovered.

To what degree the observed consumption rate differences translate to what happens *in situ* needs to be carefully evaluated. Our fecal enrichment approach was designed to probe bacterial competitive ability in the

relevant background of the full complex microbiota but by design makes specific choices of the growth environment and also neglects the host. Indeed, the consumption of succinate is dependent on a number of cofactors, in particular vitamin B₁₂ [37] and sodium [34, 36], and the specific local concentrations of these and other cofactors need not be the same in our lab setup and in humans. We do observe a decrease in succinate in all tested fecal samples, suggesting that our lab setup does allow for succinate consumption to occur, even though some of D-succinotype enrichment replicates did not consume succinate within the observation window. A more conservative interpretation of the difference in consumption rates is that *Phascolarctobacterium* has a more robust succinate consumption system than *Dialister* and is thus less dependent on externally supplied cofactors and conditions. Nevertheless, the observed higher fecal succinate concentrations in D-succinotype individuals compared to P-succinotypes despite equal population sizes is at least compatible with an *in vivo* difference in consumption rate.

Our results provide a rare mechanistic link between microbiome composition and function, and are a basis on which to functionally interpret compositional dysbiosis in disease. Differential abundances of both *Phascolarctobacterium* and *Dialister* have been independently reported as associated with IBD but have mostly not been interpreted together. The first analyses of the OSCCAR and PRISM cohorts already reported *Phascolarctobacterium* as one of the two only genera that were significantly reduced in UC and CD patients [38] with no specific mention of *Dialister*, an observation independently confirmed in other cohorts [39, 40]. Subsequent studies also reported concomitant decreased abundances of *Phascolarctobacterium* and increased *Dialister* between IBD patients and healthy controls [40, 41]. While these studies did point into the direction of a role of intestinal succinate in IBD, our classification into functionally different succinotypes now allows for a mechanistic interpretation of these consistent signals.

Attempting to classify human microbiota into different types is not new, the most prominent example being the “enterotypes” [42, 43]. Our succinotype classification differs from the enterotype classification in an important way: succinotypes are primarily informed by a functional phenotype, while enterotypes are informed by statistical differentiation of microbiome composition. While such statistical classification can be useful to reduce complex compositional differences into a simple grouping, there is *per se* no direct interpretation of what this grouping means. In contrast, the two succinotypes we describe here are based on succinate consumption rate and thus can be directly interpreted.

Finally, the succinotype classification allows for a robust stratification of patients based on a clinically relevant feature. Clinical parameters can then be tested for association with disease. In our analysis, for example, fecal succinate concentrations are higher in IBD patients compared to healthy controls, but this difference is better explained by succinotype rather than disease status. Such biomarker-based patient stratification is a powerful tool to inform treatment decisions and ultimately improve treatment outcomes.

Methods

Stool collection

The research project was approved by the Ethic Committee of the Canton of Zurich (2017-01290). Fresh fecal samples were donated from 13 healthy individuals with no history of antibiotic use, intestinal infections, or severe diarrhea during the 3 months prior to making the donation. The donors did not take immunosuppressive drugs, blood thinners, or medication affecting the bowel passage or digestion. Fecal samples were anaerobically transported in an airtight container together with an Oxoid™ AnaeroGen™ 2.5 L sachet (Thermo Fisher Diagnostics AG, Pratteln, Switzerland) and processed within 3 h after defecation. Stool consistency was evaluated optically according to the Bristol Stool Scale [44], and samples within the defined range of a healthy stool, notably with a score between 3 and 5, were accepted.

Preparation of anaerobic culture media

The growth medium was adapted from the M2GSC medium [45] for the in vitro enrichments of complex cultures as in Anthamatten et al. [22] and additionally also from YCFA [46] for single cultures. Briefly, in contrast to the common M2GSC and YCFA media, our basal medium did not contain any specific carbon sources, i.e., no glucose, starch, or cellobiose and had reduced concentrations of ampicillin (1 g/L), yeast extract (1.25 g/L), and meat extract (0.5 g/L). All medium ingredients except sodium bicarbonate and L-cysteine HCl were dissolved in an Erlenmeyer flask, and the pH was adjusted to pH 7 using 5 mM sodium hydroxide. The media were boiled for 15 min under constant moderate stirring to removal of oxygen and using a Liebig condenser to prevent vaporization of ingredients. After boiling, the media were constantly flushed with CO₂. Sodium bicarbonate and L-cysteine hydrochloride monohydrate were added when the media had cooled to 55 °C for further reduction of residual oxygen for 10 min. Aliquots of 8 mL of medium were filled into Hungate tubes under constant flushing with CO₂, and Hungate tubes were sealed with butyl rubber stoppers and screw caps (Millan SA, Geneva,

Switzerland). The media were subsequently sterilized by autoclaving and stored at room temperature.

Stool processing

The fecal samples were transferred into an anaerobic chamber (10% CO₂, 5% H₂, and 85% N₂) (Coy Laboratories, Ann Arbor, MI, USA). One gram of fecal sample measured with a sterile plastic spoon (VWR International, Dietikon, Switzerland) was suspended in 9 mL of anaerobic dilution solution (ADS). The dilution step was repeated and 1 mL of the resulting 100-fold dilution was transferred into 9 mL of ADS in a sterile Hungate tube. Serial dilutions down to 10⁻¹¹ were continued outside of the anaerobic chamber under sterile anaerobic conditions using the Hungate technique to determine the total viable cells after transport using the most probably number method.

Batch enrichments in succinate-rich conditions

Anaerobic in vitro enrichments were performed in Hungate tubes sealed with butyl rubber stoppers and screw caps (Millan SA, Geneva, Switzerland). For each enrichment, 0.3 mL of the 10⁻⁸ fecal sample dilution was inoculated into 8 mL of cultivation medium in Hungate tubes. Enrichments were performed for each of the 13 studied microbiota in three replicate cultures in a basal medium supplemented with 30 mM of disodium succinate and in a non-supplemented control condition. The media were buffered at an initial pH of 6.5. All cultures were incubated at 37 °C for up to 7 days. The optical densities were measured at 600 nm directly in the Hungate tubes with a WPA CO 8000 Cell Density Meter (Biochrom Ltd, Cambridge, England).

Microbial metabolite analysis

Succinate concentrations were measured by HPLC analysis. Samples were prepared from 1 mL of bacterial culture centrifuged at 14,000 g for 10 min at 4 °C. The supernatant was filtered into 2 mL short thread vials with crimp caps (VWR International GmbH, Schlieren, Switzerland) using non-sterile 0.2 µm regenerated cellulose membrane filters (Phenomenex Inc., Aschaffenburg, Germany). A volume of 40 µL of sample was injected into the HPLC with a flow rate of 0.6 mL/min at a constant column temperature of 80 °C and using a mixture of H₂SO₄ (10 mM) and Na-azide (0.05 g/L) as eluent. Analyses were performed with a Hitachi Chromaster 5450 RI-Detector (VWR International GmbH, Schlieren, Switzerland) using a Rezex ROA-Organic Acid (4 %) precolumn connected to a Rezex ROA-Organic Acid (8 %) column, equipped with a Security Guard Carbo-H cartridge (4 × 3 mm). Metabolite concentrations were determined using external standards (all purchased from Sigma-Aldrich,

Buchs, Switzerland) via comparison of the retention times. Peaks were integrated using the EZChromElite software (Version V3.3.2.SP2, Hitachi High Tech Science Corporation).

DNA extractions and compositional profiling by 16S metagenomic sequencing

The total genomic DNA was extracted from 200 mg of stool or from pellets of 1 mL culture (centrifuged at 14,000 g for 10 min at 4 °C), using the Maxwell[®]RSC PureFood GMO and Authentication Kit. The quality of all DNA extracts was confirmed on a Tris-Acetate-EDTA (TAE)-1.5 % agarose gel. The total DNA concentration after extraction was quantified using the Qubit[®]dsDNA HS Assay kit. We performed amplicon sequencing of the 16S rRNA V3-V4 region on Illumina MiSeq (2x 300 bp) using the primer combination 341F (5'-CCTACGGGN-BGCASCAG-3') and 806bR (5'-GGACTACNVGGG TWTCTAAT-3'). Library preparation and sequencing was performed by StarSEQ GmbH (Mainz, Germany) with 25 % PhiX. Amplicon sequence variants (ASVs) were inferred using Dada2 v1.18.0. Forward and reverse reads shorter than 250 and 210 were filtered. The maximum number of expected errors was set to 4 and 5 for forward and reverse reads, respectively. Inference was performed in "pseudo pool" mode. Read pairs were merged with a minimum overlap of 20, and chimeras were removed using the "consensus" method. After processing, the median number of reads per sample was 22,716 with an IQR of 17,937–27,904. Taxonomic annotation was done with the RDP classifier of Dada2 using the GTDB r95 database [47].

Succinate-specific enrichment

We first determined the genus-level composition of each of the succinate supplemented (SU) and non-supplemented (SU-) enrichment cultures based on 16S amplicon sequencing. To this end, we computed the regularized genus-level relative abundance by grouping all ASVs that were taxonomically classified as the same genus and normalizing the genus-specific read counts by the total read count in the sample after adding a pseudo-count of 1 if a specific genus had at least one count in the fecal sample or any derived enrichment culture. Note that in a Bayesian interpretation, the pseudo-count of 1 corresponds to a flat Dirichlet prior in a Dirichlet-Multinomial model for read counts. To account for unspecific growth, we determined maximum regularized relative abundance of a genus in the SU- enrichments. We defined the succinate-specific enrichment as the difference in regularized relative abundance of the genus in the SU cultures minus the unspecific growth.

We tested for associations of genera with succinate consumption categories of the fecal microbiota using a statistical approach. We first filtered for those genera for which the maximum succinate enrichment across all enrichments was at least 0.01, yielding 35 out of a total of 292 genera. With these 35 genera, we then performed a joint linear regression of the enrichment score on the interaction of consumption category, day, and genus with no intercept. This tests, for each combination genus, category, and day, whether the succinate enrichment is statistically different from zero. We then selected those genera with $p < 0.05$ and an estimated mean larger than zero. Using this approach we identified the four genera *Phascolarctobacterium*, *Phascolarctobacterium_A*, *Dialister*, and *Flavonifractor*.

Identification of the mmdA gene and succinate pathway

The goal was to broadly identify putative succinate consumers based on the similarity to the mmdA gene of the *Veillonella parvula* succinate-to-propionate cluster (UniProt Q57079). We first looked for putative hits in all translated genomes from GTDB release 214 with phmmer (HMMER 3.3) and filtered for those with an e -value below 10^{-150} , resulting in 1643 distinct genomes. For each genus, we kept only the hit with the lowest e -value, leaving 281 distinct genera. We then performed multiple sequence alignment with MAFFT [48] 7.453 including the human PCCB gene to use as a phylogenetic outgroup. Finally, we reconstructed the phylogeny of mmdA genes using RAXML-NG [49] 1.2.0 with a JTT+G model, 10 maximum parsimony starting trees, and 200 bootstraps. For representative genomes of the four succinate utilizers (GCA_000160055.1, GCA_003945365.1, GCA_010508875.1, GCA_023497905.1), we identified the succinate-to-propionate gene cluster using gutSMASH [50].

Testing of isolates for succinate consumption

Strains were pre-cultured in M2GSC medium, with the exception of *Akkermansia muciniphila* DSMZ 22959 that was pre-cultured in M2-based medium supplemented with 3 g/L of type II mucin (Sigma-Aldrich Chemie GmbH, Buchs, Switzerland) and *Veillonella parvula* DSMZ 2008 that was pre-cultured in M2-based medium supplemented with 60mM of DL-lactic acid 90% (Sigma-Aldrich Chemie GmbH, Buchs, Switzerland). To test for succinate consumption, we inoculated 0.1 mL of 48 h pre-cultures into 8 mL of M2-based medium supplemented with 30 mM or 80 mM of succinate and quantified the succinate concentrations after 2 and 7 days.

Cultures for succinate consumption kinetics

The strains to be tested were pre-cultured in YCFA medium supplemented with 80mM of succinate. To standardize the starting cell densities, we quantified the cell concentrations of the pre-cultures by flow cytometry using live/dead staining. A double staining assay with the two nucleic acid dyes SYBR Green (SG) and propidium iodide (PI) was used to differentiate between cells with intact (viable) and damaged (dead) cytoplasmic membranes [51]. We aimed for a starting cell density of 1×10^7 cells/mL; if necessary, pre-cultures were diluted accordingly in anaerobic dilution solution.

Cultures were performed in 8 mL of YCFA medium supplemented with 80 mM of succinate. We selected sampling times for the different strains based on preliminary growth test in order to target the time window where most of the succinate consumption occurs: 1 h intervals during 25 h for *Phascolarctobacterium*, 2 h intervals during 52 h for *Flavonifractor*, and 4 h intervals during 100 h for *Dialister*. Separate cultures were inoculated for each time point to avoid effects from repeated sampling and full duplicates using separate pre-cultures.

Estimation of the per capita succinate consumption rate

We modeled succinate uptake following Monod,

$$\frac{dA}{dt} = -\mu \frac{A}{K+A} x, \quad (1)$$

$$\frac{dx}{dt} = -\phi \frac{dA}{dt}, \quad (2)$$

where $A(t)$ is the concentration of substrate and $x(t)$ is the microbial density at time t . μ is the maximum *per capita* succinate uptake rate, and ϕ is the growth yield per unit succinate taken up.

We then estimate the parameters μ , ϕ , and K using Bayesian Markov Chain Monte Carlo (MCMC) using Stan [52, 53]. For each sample of the parameters, we first numerically solve the system of ordinary differential Eqs. (1) and (2) with $A(0) = A_0$ and $x(0) = x_0$. We then compute the log-likelihood of the observed data using the following hierarchical model,

$$\begin{aligned} X(t) &\sim \mathcal{N}(x(t), s_x), \\ A(t) &\sim \mathcal{N}(A(t), s_A), \end{aligned}$$

where \mathcal{N} signifies the normal distribution, with the parameters sampled from the following prior distributions unless otherwise specified,

$$\begin{aligned} s_x &\sim \mathcal{N}(0, 0.001), \quad s_x \geq 0, \\ s_A &\sim \mathcal{N}(0, 0.01), \quad s_A \geq 0, \\ \mu &\sim \mathcal{N}(50, 2), \quad \mu \geq 0, \\ \ln \phi &\sim \mathcal{N}(-2, 0.3), \\ K &\sim \mathcal{N}(20, 3), \quad K \geq 0, \\ \ln x_0 &\sim \mathcal{N}(0.004, 0.1), \\ \ln A_0 &\sim \mathcal{N}(80, 0.03). \end{aligned}$$

We use the Runge-Kutta (4,5) method as implemented in CmdStan to solve the system of ODEs. Summary statistics for the sampled parameters and convergence diagnostics are listed in Supplementary Text S1.

To account for bacterial growth on a first (unobserved) preferential substrate, we modified Eqs. (1) and (2) to include a relative allocation into the uptake of a preferential substrate, B , and a secondary substrate, A . For simplicity, we use the affinity fraction, $B/(K_B + B)$, from the Monod equations as the switch between substrates,

$$\frac{dA}{dt} = -\mu_A \frac{A}{K+A} \left(1 - \frac{B}{K_B+B}\right) x, \quad (3)$$

$$\frac{dB}{dt} = -\mu_B \frac{B}{K_B+B} x, \quad (4)$$

$$\frac{dx}{dt} = -\phi_B \frac{dB}{dt} - \phi_A \frac{dA}{dt}. \quad (5)$$

We then estimated the parameters in an analogous MCMC approach as the simpler model, with the additional or modified priors,

$$\begin{aligned} \mu_A &\sim \mathcal{N}(50, 10), \quad \mu_A \geq 0, \\ \mu_B &\sim \mathcal{N}(100, 40), \quad \mu_B \geq 0, \\ \ln \phi_B &\sim \mathcal{N}(-2, 0.3), \\ K_B &\sim \mathcal{N}(20, 3), \quad K_B \geq 0. \end{aligned}$$

Because the concentration of the substrate B is not observed, we cannot estimate the values of B_0 , which we set to $B_0 = 100$ without loss of generality. This implies that the value of B and thus also μ_B , ϕ_B , and K_B are in arbitrary units.

Other amplicon and shotgun metagenomic data

For the American Gut Project [24], we downloaded the sOTU tables and corresponding DNA sequences from figshare and performed a new taxonomic assignment with the GTDB r95 database and the RDP classifier from Dada2. For the PROTECT [27] and UCC [25] data, we downloaded the raw sequencing reads from NCBI PRJNA436359 and PRJNA414072 and inferred ASVs and performed taxonomic assignment using the

same pipeline as for the enrichment data. Additionally, we fetched those datasets from the “gut microbiome-metabolome dataset collection” [31] that were based on 16S amplicon data [23, 26, 54–56] and directly used the ASV counts and GTDB taxonomic assignments.

For the shotgun metagenomic data, we fetched all datasets from the curatedMetagenomicData [28] for which relative abundance were computed and used the provided taxonomic assignments. Additionally, we also fetched the compositional and metabolomic data for PRISM [30] cohort from the “gut microbiome-metabolome dataset collection.”

Supplementary Information

The online version contains supplementary material available at <https://doi.org/10.1186/s40168-024-01897-8>.

Supplementary Material 1

Acknowledgements

We thank Leandra Knecht for support with experimental work, Alice de Wouters and Shaul Pollak for feedback and discussions, and Jill Marie O’Sullivan for uncovering additional studies reporting differential abundances of P and D. We also thank the AVINA Foundation for support.

Authors’ contributions

L.A., C.M., and J.Z. performed experiments. L.A., T.d.W., and G.E.L. planned the execution of the project. L.A., P.R.v.B., and G.E.L. analyzed the data. L.A., T.d.W., and G.E.L. conceived the project. L.A., C.L., T.d.W., and G.E.L. interpreted the results. G.E.L. and L.A. wrote the first draft of the manuscript. All authors reviewed the final manuscript and provided feedback.

Funding

PharmaBiome provided financial support and was supported by a grant from the AVINA foundation.

Data availability

The raw sequencing data is available at the European Genome-Phenome Archive in dataset EGAD5000000740. All details related to the analysis methods are in the main text or supplementary materials.

Declarations

Ethics approval and consent to participate

The research project was approved by the Ethic Committee of the Canton of Zurich (2017-01290).

Consent for publication

Not applicable.

Competing interests

L.A., P.R.v.B., C.M., T.d.W., and G.E.L. are or were employees of PharmaBiome. T.d.W. and C.L. are founders of PharmaBiome. L.A. is a co-founder of PharmaBiome. L.A., P.R.v.B., T.d.W., and G.E.L. are inventors on the patent application WO 2022/023458 A1 entitled “Microbial Niche Mapping” and on the patent application WO 2023/118460 A1 entitled “New biomarker for disorders and diseases associated with intestinal dysbiosis”. PharmaBiome provided financial support.

Received: 29 November 2023 Accepted: 31 July 2024

Published online: 30 September 2024

References

- Fan Y, Pedersen O. Gut microbiota in human metabolic health and disease. *Nat Rev Microbiol*. 2021;19(1):55–71. <https://doi.org/10.1038/s41579-020-0433-9>.
- Cox TO, Lundgren P, Nath K, Thaiss CA. Metabolic control by the microbiome. *Genome Med*. 2022;14(1):80. <https://doi.org/10.1186/s13073-022-01092-0>.
- Fernández-Veledo S, Vendrell J. Gut microbiota-derived succinate: friend or foe in human metabolic diseases? *Rev Endocr Metab Disord*. 2019;20(4):439–47. <https://doi.org/10.1007/s11154-019-09513-z>.
- Watanabe Y, Nagai F, Morotomi M. Characterization of *Phascolarctobacterium succinatutens* sp. nov., an Asaccharolytic, Succinate-Utilizing Bacterium Isolated from Human Feces. *Appl Environ Microbiol*. 2012;78(2):511–518. <https://doi.org/10.1128/aem.06035-11>.
- Louis P, Flint HJ. Formation of propionate and butyrate by the human colonic microbiota. *Environ Microbiol*. 2017;19(1):29–41. <https://doi.org/10.1111/1462-2920.13589>.
- Connors J, Dawe N, Limbergen JV. The role of succinate in the regulation of intestinal inflammation. *Nutrients*. 2018;11(1):25. <https://doi.org/10.3390/nu11010025>.
- Topping DL, Clifton PM. Short-chain fatty acids and human colonic function: roles of resistant starch and nonstarch polysaccharides. *Physiol Rev*. 2001;81(3):1031–64. <https://doi.org/10.1152/physrev.2001.81.3.1031>.
- Vernia P, Caprilli R, Latella G, Barbetti F, Magliocca FM, Cittadini M. Fecal lactate and ulcerative colitis. *Gastroenterology*. 1988;95(6):1564–8. [https://doi.org/10.1016/s0016-5085\(88\)80078-7](https://doi.org/10.1016/s0016-5085(88)80078-7).
- Woodmansey EJ, McMurdo MET, Macfarlane GT, Macfarlane S. Comparison of compositions and metabolic activities of fecal microbiotas in young adults and in antibiotic-treated and non-antibiotic-treated elderly subjects. *Appl Environ Microbiol*. 2004;70(10):6113–22. <https://doi.org/10.1128/aem.70.10.6113-6122.2004>.
- Rubic T, Lametschwandtner G, Jost S, Hinteregger S, Kund J, Carballido-Perrig N, et al. Triggering the succinate receptor GPR91 on dendritic cells enhances immunity. *Nat Immunol*. 2008;9(11):1261–9. <https://doi.org/10.1038/ni.1657>.
- Macias-Ceja DC, Ortiz-Masiá D, Salvador P, Gisbert-Ferrández L, Hernández C, Hausmann M, et al. Succinate receptor mediates intestinal inflammation and fibrosis. *Mucosal Immunol*. 2019;12(1):178–87. <https://doi.org/10.1038/s41385-018-0087-3>.
- Serena C, Monfort-Ferre D, Bautista M, Menacho M, Marti M, Espin E, et al. P001 Succinate, a gut microbiota-derived metabolite, modulates the inflammatory status of the creeping fat in Crohn’s disease. *J Crohn’s Colitis*. 2021;15(Supplement_1):S123–S123. <https://doi.org/10.1093/ecco-jcc/jjab076.130>.
- Zakerska-Banaszak O, Tomczak H, Gabryel M, Baturo A, Wolko L, Michalak M, et al. Dysbiosis of gut microbiota in Polish patients with ulcerative colitis: a pilot study. *Sci Rep*. 2021;11(1):2166. <https://doi.org/10.1038/s41598-021-81628-3>.
- Reichardt N, Duncan SH, Young P, Belenguer A, Leitch CM, Scott KP, et al. Phylogenetic distribution of three pathways for propionate production within the human gut microbiota. *ISME J*. 2014;8(6):1323–35. <https://doi.org/10.1038/ismej.2014.14>.
- Flint HJ, Duncan SH, Scott KP, Louis P. Links between diet, gut microbiota composition and gut metabolism. *Proc Nutr Soc*. 2015;74(1):13–22. <https://doi.org/10.1017/s0029665114001463>.
- Fischbach MA, Sonnenburg JL. Eating for two: how metabolism establishes interspecies interactions in the gut. *Cell Host Microbe*. 2011;10(4):336–47. <https://doi.org/10.1016/j.chom.2011.10.002>.
- Janssen PH. Growth yield increase and ATP formation linked to succinate decarboxylation in *Veillonella parvula*. *Arch Microbiol*. 1992;157(5):442–5. <https://doi.org/10.1007/bf00249102>.
- Dot TD, Osawa R, Stackebrandt E. *Phascolarctobacterium faecium* gen. nov., spec. nov., a Novel Taxon of the Sporomusa Group of Bacteria. *Syst Appl Microbiol*. 1993;16(3):380–384. [https://doi.org/10.1016/s0723-2020\(11\)80269-9](https://doi.org/10.1016/s0723-2020(11)80269-9).
- Jumas-Bilak E, Jean-Pierre H, Carlier JP, Teysier C, Bernard K, Gay B, et al. *Dialister microaerophilus* sp. nov. and *Dialister propionicifaciens* sp. nov., isolated from human clinical samples. *Int J Syst Evol Microbiol*. 2005;55(6):2471–2478. <https://doi.org/10.1099/ijso.0.63715-0>.

20. Morotomi M, Nagai F, Sakon H, Tanaka R. *Dialister succinatiphilus* sp. nov. and *Barnesiella intestinihominis* sp. nov., isolated from human faeces. *Int J Syst Evol Microbiol*. 2008;58(12):2716–2720. <https://doi.org/10.1099/ijs.0.2008/000810-0>.
21. Sakamoto M, Ikeyama N, Toyoda A, Murakami T, Mori H, Iino T, et al. *Dialister hominis* sp. nov., isolated from human faeces. *Int J Syst Evol Microbiol*. 2020;70(1):589–595. <https://doi.org/10.1099/ijsem.0.003797>.
22. Anthamatten L, Bieberstein PRV, Thabuis C, Menzi C, Reichlin M, Meola M, et al. Mapping gut bacteria into functional niches reveals the ecological structure of human gut microbiomes. *bioRxiv*. 2023. <https://doi.org/10.1101/2023.07.04.547750>.
23. Jacobs JP, Goudarzi M, Singh N, Tong M, McHardy IH, Ruegger P, et al. A disease-associated microbial and metabolomics state in relatives of pediatric inflammatory bowel disease patients. *Cell Mol Gastroenterol Hepatol*. 2016;2(6):750–66. <https://doi.org/10.1016/j.jcmgh.2016.06.004>.
24. McDonald D, Hyde E, Debelius JW, Morton JT, Gonzalez A, Ackermann G, et al. American Gut: an open platform for citizen science microbiome research. *mSystems*. 2018;3(3):e00031–18. <https://doi.org/10.1128/msystems.00031-18>.
25. Clooney AG, Eckenberger J, Laserna-Mendieta E, Sexton KA, Bernstein MT, Vagianos K, et al. Ranking microbiome variance in inflammatory bowel disease: a large longitudinal intercontinental study. *Gut*. 2021;70(3):499–510. <https://doi.org/10.1136/gutjnl-2020-321106>.
26. Poyet M, Groussin M, Gibbons SM, Avila-Pacheco J, Jiang X, Kearney SM, et al. A library of human gut bacterial isolates paired with longitudinal multiomics data enables mechanistic microbiome research. *Nat Med*. 2019;25(9):1442–52. <https://doi.org/10.1038/s41591-019-0559-3>.
27. Schirmer M, Denson L, Vlamakis H, Franzosa EA, Thomas S, Gotman NM, et al. Compositional and temporal changes in the gut microbiome of pediatric ulcerative colitis patients are linked to disease course. *Cell Host Microbe*. 2018;24(4):600–610.e4. <https://doi.org/10.1016/j.chom.2018.09.009>.
28. Pasolli E, Schiffer L, Manghi P, Renson A, Obenchain V, Truong DT, et al. Accessible, curated metagenomic data through ExperimentHub. *Nat Med*. 2017;14(11):1023–4. <https://doi.org/10.1038/nmeth.4468>.
29. Parks DH, Chuvpochina M, Waite DW, Rinke C, Skarshewski A, Chaumeil PA, et al. A standardized bacterial taxonomy based on genome phylogeny substantially revises the tree of life. *Nat Biotechnol*. 2018;36(10):996–1004. <https://doi.org/10.1038/nbt.4229>.
30. Franzosa EA, Sirota-Madi A, Avila-Pacheco J, Fornelos N, Haiser HJ, Reinker S, et al. Gut microbiome structure and metabolic activity in inflammatory bowel disease. *Nat Microbiol*. 2019;4(2):293–305. <https://doi.org/10.1038/s41564-018-0306-4>.
31. Muller E, Algavi YM, Borenstein E. The gut microbiome-metabolome dataset collection: a curated resource for integrative meta-analysis. *NPJ Biofilms Microbiomes*. 2022;8(1):79. <https://doi.org/10.1038/s41522-022-00345-5>.
32. Ferreyra JA, Wu KJ, Hryckowian AJ, Bouley DM, Weimer BC, Sonnenburg JL. Gut microbiota-produced succinate promotes *C. difficile* infection after antibiotic treatment or motility disturbance. *Cell Host Microbe*. 2014;16(6):770–777. <https://doi.org/10.1016/j.chom.2014.11.003>.
33. Kenealy WR, Waselefsky DM. Studies on the substrate range of *Clostridium kluyveri*; the use of propanol and succinate. *Arch Microbiol*. 1985;141(3):187–94. <https://doi.org/10.1007/bf00408056>.
34. Janssen PH, Liesack W, Kluge C, Seeliger S, Schink B, Harfoot CG. Sodium-dependent succinate decarboxylation by a new anaerobic bacterium belonging to the genus *Peptostreptococcus*. *Antonie Van Leeuwenhoek*. 1996;70(1):11–20. <https://doi.org/10.1007/bf00393565>.
35. Caspari D, Macy JM. The role of carbon dioxide in glucose metabolism of *Bacteroides fragilis*. *Arch Microbiol*. 1983;135(1):16–24. <https://doi.org/10.1007/bf00419476>.
36. Schink B, Pfennig N. *Propionigenium modestum* gen. nov. sp. nov. a new strictly anaerobic, nonsporulating bacterium growing on succinate. *Arch Microbiol*. 1982;133(3):209–216. <https://doi.org/10.1007/bf00415003>.
37. Stadtman ER, Overath P, Eggerer H, Lynen F. The role of biotin and vitamin B12 coenzyme in propionate metabolism. *Biochem Biophys Res Commun*. 1960;2(1):1–7. [https://doi.org/10.1016/0006-291x\(60\)90252-7](https://doi.org/10.1016/0006-291x(60)90252-7).
38. Morgan XC, Tickle TL, Sokol H, Gevers D, Devaney KL, Ward DV, et al. Dysfunction of the intestinal microbiome in inflammatory bowel disease and treatment. *Genome Biol*. 2012;13(9):R79. <https://doi.org/10.1186/gb-2012-13-9-r79>.
39. Bajer L, Kverka M, Kostovcik M, Macinga P, Dvorak J, Stehlikova Z, et al. Distinct gut microbiota profiles in patients with primary sclerosing cholangitis and ulcerative colitis. *World J Gastroenterol*. 2017;23(25):4548–58. <https://doi.org/10.3748/wjg.v23.i25.4548>.
40. Kim CH, Lee YU, Kim KH, Kang S, Kang GH, Chu H, et al. Comparison of metabolites and gut microbes between patients with ulcerative colitis and healthy individuals for an integrative medicine approach to ulcerative colitis—a pilot observational clinical study (STROBE compliant). *Diagnostics*. 2022;12(8):1969. <https://doi.org/10.3390/diagnostics12081969>.
41. Paljetak HČ, Barešić A, Panek M, Perić M, Matijašić M, Lojkić I, et al. Gut microbiota in mucosa and feces of newly diagnosed, treatment-naïve adult inflammatory bowel disease and irritable bowel syndrome patients. *Gut Microbes*. 2022;14(1):2083419. <https://doi.org/10.1080/19490976.2022.2083419>.
42. Arumugam M, Raes J, Pelletier E, Paslier DL, Yamada T, Mende DR, et al. Enterotypes of the human gut microbiome. *Nature*. 2011;473(7346):174–80. <https://doi.org/10.1038/nature09944>.
43. Costea PI, Hildebrand F, Arumugam M, Bäckhed F, Blaser MJ, Bushman FD, et al. Enterotypes in the landscape of gut microbial community composition. *Nat Microbiol*. 2018;3(1):8–16. <https://doi.org/10.1038/s41564-017-0072-8>.
44. Lewis SJ, Heaton KW. Stool form scale as a useful guide to intestinal transit time. *Scand J Gastroenterol*. 1997;32(9):920–4. <https://doi.org/10.3109/00365529709011203>.
45. Miyazaki K, Martin JC, Marinsek-Logar R, Flint HJ. Degradation and utilization of xylans by the Rumen Anaerobe *Prevotella bryantii* (formerly *P. ruminicola* subsp. *brevis*) B14. *Anaerobe*. 1997;3(6):373–381. <https://doi.org/10.1006/anae.1997.0125>.
46. Duncan SH, Hold GL, Harmsen HJM, Stewart CS, Flint HJ. Growth requirements and fermentation products of *Fusobacterium prausnitzii*, and a proposal to reclassify it as *Faecalibacterium prausnitzii* gen. nov., comb. nov. *Int J Syst Evol Microbiol*. 2002;52(6):2141–2146. <https://doi.org/10.1099/00207713-52-6-2141>.
47. Alishum A. DADA2 formatted 16S rRNA gene sequences for both bacteria & archaea. Bash script can be provided on request. Zenodo; 2022. <https://doi.org/10.5281/zenodo.6655692>.
48. Katoh K, Standley DM. MAFFT Multiple Sequence Alignment Software Version 7: improvements in performance and usability. *Mol Biol Evol*. 2013;30(4):772–80. <https://doi.org/10.1093/molbev/mst010>.
49. Kozlov AM, Darriba D, Flouri T, Morel B, Stamatakis A. RAxML-NG: a fast, scalable, and user-friendly tool for maximum likelihood phylogenetic inference. *Bioinformatics*. 2019;35(21):4453–5. <https://doi.org/10.1093/bioinformatics/btz305>.
50. Andreu VP, Augustijn HE, Chen L, Zhernakova A, Fu J, Fischbach MA, et al. gutSMASH predicts specialized primary metabolic pathways from the human gut microbiota. *Nat Biotechnol*. 2023;1–8. <https://doi.org/10.1038/s41587-023-01675-1>.
51. Nevel SV, Koetzsch S, Weilenmann HU, Boon N, Hammes F. Routine bacterial analysis with automated flow cytometry. *J Microbiol Meth*. 2013;94(2):73–6. <https://doi.org/10.1016/j.mimet.2013.05.007>.
52. Stan Development Team. Stan Modeling Language Users Guide and Reference Manual. 2023. <https://mc-stan.org>.
53. Gabry J, Češnovar R, Johnson A. cmdstanr: R Interface to 'CmdStan'. 2023. <https://mc-stan.org/cmdstanr>.
54. Kang DW, Ilhan ZE, Isern NG, Hoyt DW, Howsmon DP, Shaffer M, et al. Differences in fecal microbial metabolites and microbiota of children with autism spectrum disorders. *Anaerobe*. 2018;49:121–31. <https://doi.org/10.1016/j.anaerobe.2017.12.007>.
55. Kim M, Vogtmann E, Ahlquist DA, Devens ME, Kisiel JB, Taylor WR, et al. Fecal metabolomic signatures in colorectal adenoma patients are associated with gut microbiota and early events of colorectal cancer pathogenesis. *mBio*. 2020;11(1):e03186–19. <https://doi.org/10.1128/mbio.03186-19>.
56. Kostic AD, Gevers D, Siljander H, Vatanen T, Hyötyläinen T, Hämäläinen AM, et al. The dynamics of the human infant gut microbiome in development and in progression toward type 1 diabetes. *Cell Host Microbe*. 2015;17(2):260–73. <https://doi.org/10.1016/j.chom.2015.01.001>.

Publisher's Note

Springer Nature remains neutral with regard to jurisdictional claims in published maps and institutional affiliations.